

# Exocomet signatures around the A-shell star $\phi$ Leo?

C. Eiroa<sup>1</sup>, I. Rebollido<sup>1</sup>, B. Montesinos<sup>2</sup>, E. Villaver<sup>1</sup>, O. Absil<sup>3</sup>, Th. Henning<sup>4</sup>, A. Bayo<sup>5</sup>, H. Canovas<sup>1</sup>, A. Carmona<sup>6</sup>, Ch. Chen<sup>7</sup>, S. Ertel<sup>8</sup>, D. P. Iglesias<sup>5</sup>, R. Launhardt<sup>4</sup>, J. Maldonado<sup>9</sup>, G. Meeus<sup>1</sup>, A. Moór<sup>10</sup>, A. Mora<sup>11</sup>, A. J. Mustill<sup>12</sup>, J. Olofsson<sup>5</sup>, P. Riviere-Marichalar<sup>13</sup>, and A. Roberge<sup>14</sup>

(Affiliations can be found after the references)

## ABSTRACT

We present an intensive monitoring of high-resolution spectra of the Ca II K line in the A7IV shell star  $\phi$  Leo at very short (minutes, hours), short (night to night), and medium term (weeks, months) timescales. The spectra show remarkable variable absorptions on timescales of hours, days and months. The characteristics of these sporadic events are very similar to most of the ones observed towards the debris disk host star  $\beta$  Pic, which are usually interpreted as signs of the evaporation of solid, comet-like bodies grazing or falling onto the star. Therefore, our results suggest the presence of solid bodies around  $\phi$  Leo. To our knowledge, with the exception of  $\beta$  Pic, our monitoring is the one with the best time resolution at the mentioned timescales done on a star with events attributed to exocomets. Assuming the cometary scenario, and considering the timescales of our monitoring, our results point to  $\phi$  Leo presenting the richest environment with comet-like events yet known, second only to  $\beta$  Pic.

**Key words.** planetary systems – stars: individual:  $\phi$  Leo – comets: general – circumstellar matter

## 1. Introduction

In spite of their low mass, Kuiper Belt objects, comets and asteroids are key elements to understand the early history of the Solar System, its dynamics and composition. While exoplanets are now routinely detected and hundreds of debris disks provide indirect evidence of planetesimals around main-sequence (MS) stars (Matthews et al. 2014), little is directly known about minor bodies around other stars than the Sun. The immense difficulty of a direct detection resides on the fact that they lack a large surface area required to detect their thermal or scattered emission. Dust features provide hints about the properties of  $\mu\text{m}$ -size grains in debris disks resulting from collisions of planetesimals (e.g. Olofsson et al. 2012). Circumstellar (CS) CO emission around some AF-type MS stars (e.g. Moór et al. 2015; Marino et al. 2016), has been interpreted as due to outgassing produced by comet collisions (Zuckerman & Song 2012). A complementary, somehow more direct, information on the exocomets' nature and composition is provided by the detection of variable absorptions superposed to photospheric lines in the spectra of some stars.

Variable absorption features in metallic lines have been known for around 30 years in the optical spectrum of  $\beta$  Pic (Hobbs et al. 1985). These irregular features, mainly traced in the Ca II K line, appear red- and, in a much less degree, blue-shifted with respect to the radial velocity of the star, and might vary in timescales as short as hours. They have been interpreted as due to the gas released by the evaporation of exocomets grazing or falling onto the star (Ferlet et al. 1987; Kiefer et al. 2015, and references therein), driven into the vicinity of the star by the perturbing action of a larger body, i.e. a planet (Beust et al. 1991). Such variable absorptions have also been observed towards a handful of A-type stars (e.g. Redfield et al. 2007; Roberge & Weinberger 2008; Welsh & Montgomery 2015).

We have initiated a short and medium-term high-resolution spectroscopic project aiming at detecting and monitoring such sporadic events attributed to exocomets in a sample of MS stars,

most of them A-type but also some FG-type with a range of ages. The sample includes stars for which exocomets' signatures have already been detected, e.g. 49 Ceti or HR 10, as well as stars not scrutinized yet for such events. So far, we have obtained more than 1200 spectra of  $\sim 100$  stars (Rebollido et al., in preparation). Among the observed stars,  $\phi$  Leo (HR 4368, HD 98058, HIP 55084) stands out as its spectrum exhibits conspicuous variations on timescales of hours, days and months. This work presents our results concerning the Ca II K line obtained in five observing runs from December 2015 to May 2016. This line is particularly sensitive to those absorptions and is the one usually analyzed in the exocomets' literature. Results regarding other relevant lines including the Ca II IR-triplet, Ti II, Na I D and Balmer lines, together with the spectra of other stars, will be presented in a forthcoming paper.

## 2. $\phi$ Leo: properties and astrophysical parameters

$\phi$  Leo is an A7IVn shell star (Jaschek et al. 1991) located at a distance of 56.5 pc. The star is seen close to edge-on with a very high rotational velocity,  $v \sin i \sim 220 - 254$  km/s (Lagrange-Henri et al. 1990; Royer et al. 2007). It is surrounded by a gaseous CS disk detected in the Ti II 3685, 3759, 3762 Å lines as well as in the Ca II H/K lines (e.g. Jaschek et al. 1988; Abt 2008).  $\phi$  Leo is close to the center of the local interstellar bubble, a cavity of low density, which makes it unlikely that its shell/disk is formed by accretion of the interstellar medium, as conjectured for other A-shell stars (Abt 2015). The Ca II K profile shows a triangular shape probably due to the combination of the photospheric and disk absorptions (Lagrange-Henri et al. 1990). The star does not possess a warm debris disk (Rieke et al. 2005), although a cool debris disk cannot be excluded since data at  $\lambda > 25 \mu\text{m}$  are not existing to our knowledge. The best Kurucz photospheric model fitting our spectra is  $T_{\text{eff}} = 7500$  K,  $\log g = 3.75$ ,  $v \sin i = 230$  km/s, in good agreement with previous estimates (e.g. David &

arXiv:1609.04263v1 [astro-ph.SR] 14 Sep 2016

**Table 1.** Log of observations

Observing run	Dates	Spectra per night
2015 December <sup>1</sup>	20, 22, 23	1, 4, 1
2016 January <sup>1</sup>	27, 28, 30	1, 3, 3
2016 March <sup>1</sup>	3, 4, 5, 6	4, 4, 2, 3
2016 March <sup>2</sup>	25, 26, 27, 28	4, 4, 3, 3
2016 May <sup>1</sup>	11	20

<sup>1</sup> HERMES, <sup>2</sup> FEROS

Hillebrand 2015). Its bolometric luminosity is  $\sim 45 L_{\odot}$  (Zorec & Royer 2012) and age estimates are in the range  $\sim 500$ -900 Myr (David & Hillebrand 2015; De Rosa et al. 2014; Zorec & Royer 2012).

### 3. Observations

High resolution spectra of  $\phi$  Leo were obtained with the high resolution fiber-fed échelle spectrographs HERMES and FEROS attached at the Mercator (La Palma, Spain) and MPG/ESO 2.2 m (La Silla, Chile) telescopes, respectively. A total of 60 spectra of  $\phi$  Leo were taken. Observing dates, telescope, and number of spectra per night are given in Table 1. HERMES has a spectral resolution of  $\sim 85000$  (high resolution mode) covering the range  $\lambda\lambda \sim 370$ -900 nm (Raskin et al. 2011). Exposure times ranged from 260 to 600 seconds. Some spectra were taken consecutively and combined after reduction. FEROS has a spectral resolution  $R \sim 48000$  covering the range from  $\sim 350$  to 929 nm (Kaufer et al. 1999). Exposure times ranged from 120 to 360 seconds. Both HERMES and FEROS spectra have been reduced using the available pipelines of both instruments. Barycentric corrections have also been made for all spectra.

### 4. Results

Distinct changes are observed in the Ca II H and K lines of  $\phi$  Leo. Those changes affect the line profile as well as the wavelength and depth of the absorption peak. Variations happen on timescales of hours, days and months. All the spectra show the triangular shape noticed by Lagrange-Henri et al. (1990) modulated in most cases by an extra red-shifted absorption. Further, we do not identify any temporal variability pattern. In the following we will refer to the Ca II K line only, although we will also comment on some Ca II H line spectra to illustrate the results concerning this line in comparison with the K line.

#### 4.1. The “stable” Ca II K component

The Ca II K line spectra taken on 2015 December 20 and 23 are identical with its absorption peak at the stellar radial velocity,  $v_{\text{rad}} = -3$  km/s (de Bruijne & Eilers 2012). The rest of the spectra are either deeper with the absorption peak shifted to longer wavelengths, or with obvious extra red-shifted absorption components superposed to the December 20 and 23 spectra. The “exceptions” are the spectra of 2016 March 3 and 5 where small differences with those of December 20 and 23 are seen (see below).

Figure 1 shows the average of the December 20 and 23 Ca II K line together with the photospheric line of a Kurucz model with stellar parameters mentioned in Section 2. The broad, FWHM = 56 km/s, extra absorption at approximately the stellar radial velocity produces the triangular shape of the line profile. Its depth and equivalent width are 0.238 and 0.22 Å, respectively.

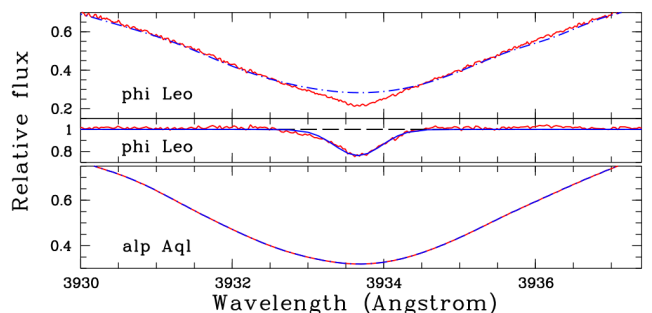


**Fig. 1.** Top: Average Ca II K line of  $\phi$  Leo from 2015 December 20 and 23 (red continuous line), together with a Kurucz photospheric model (blue dash-dot line). See text for stellar parameters. Middle: residuals of the average 20 and 23 spectra with respect to the photospheric line. The blue continuum line is a gaussian with FWHM = 56 km/s. Bottom: observed Ca II K line (red line) of  $\alpha$  Aql compared with a Kurucz model (blue dash-dot line) with stellar parameters  $T_{\text{eff}} = 7900$  K,  $\log g = 4.25$ ,  $v \sin i = 210$  km/s.

This corresponds to a column density  $N(\text{Ca II}) \sim 2.3 \times 10^{12} \text{ cm}^{-2}$ . In order to ensure that the “extra absorption” is real, we have synthesized a photospheric model for  $\alpha$  Aql, a star with similar spectral type (A7Vn) and rotational velocity, and compared it to spectra taken with the same instrument and configuration as for  $\phi$  Leo. Figure 1 shows the excellent fit of the corresponding  $\alpha$  Aql model to the observed spectra.

These results suggest that during December 20 and 23 we have detected the contribution of a CS gas disk superposed to the stellar photosphere while the rest of the spectra are affected by additional gas absorptions, although other causes producing the triangular absorption cannot be excluded (see below). In the following we assume that the extra absorption seen on December 20 and 23 is a “stable” component in addition to the  $\phi$  Leo photosphere and take the average of both spectra as a template to analyse other contributions to the gas components.

#### 4.2. The variable Ca II K components

*Mercator 2015 December.* The four spectra of December 22 show no appreciable changes but their absorption is red-shifted and deeper than the average December 20 and 23 template spectrum. Figure 2 shows the average of those four spectra, as well as the residuals taking the template spectrum as a “continuum” for the December 22 one. There is an obvious absorption event at  $v \sim 6.0$  km/s, i.e.  $\sim 9.0$  km/s red-shifted from the stellar radial velocity, and depth  $\sim 0.083$ . A second event might be present at a velocity  $\sim 16$  km/s and depth  $\sim 0.060$ . The equivalent width of both events together is  $\sim 23 \text{ m}\text{\AA}$ , and its FWHM  $\sim 25$  km/s. The figure also shows the residuals corresponding to the Ca II H; in this case only one event with a depth of  $\sim 0.054$  is clearly seen.

*Mercator 2016 January.* These spectra appear a bit red-shifted with respect to the template spectrum but their depth is lower than the one of December 22. There might be tiny changes among the spectra taken in different nights although we consider only their average because poor weather conditions produced relatively low S/N ratios. Figure 2 shows the 2016 January spectrum and its residual compared to the template. An event at  $\sim 15$  km/s, i.e. red-shifted  $\sim 18$  km/s with respect to the stellar radial velocity, is clearly discernible. Its equivalent width is  $20 \text{ m}\text{\AA}$ , depth 0.055 and FWHM  $\sim 20$  km/s.

*Mercator 2016 March.* There were no detectable variations during the individual nights but the Ca II K line clearly varied from

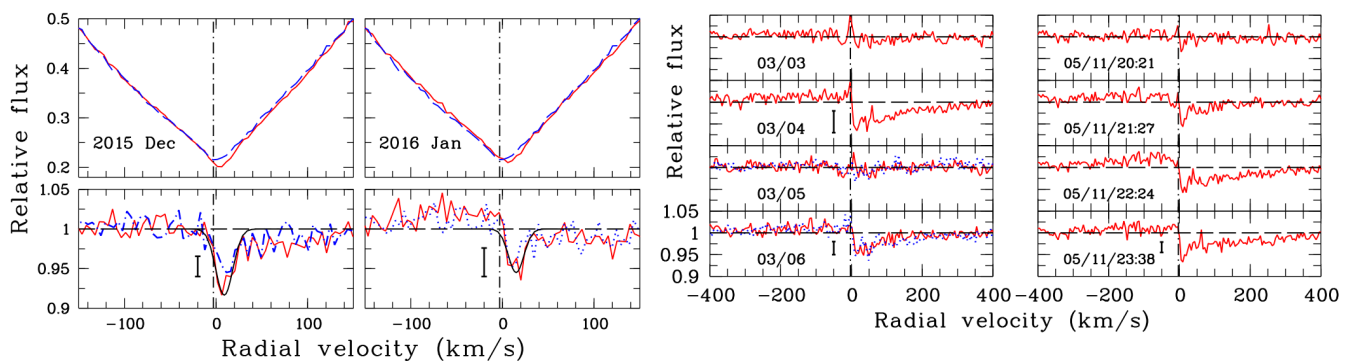


**Fig. 2.** From left to right the Ca II K line from the observing runs with Mercator. At the top of the December and January panels the average of the four December 22 spectra and the average of the January spectra are plotted (red continuous lines) together with the template spectrum (blue dashed line). At the bottom are the corresponding residuals in red. To guide the eye, two Gaussians with FWHM 25 km/s (December) and 20 km/s (January) are plotted (black continuous line). The March panel shows the residuals of the average spectrum of each night. The May panel shows the average of five consecutive spectra of May 11 starting at the UT indicated in the panel. Some panels show the residuals of the Ca II H line for comparison (blue dot line). A  $3\text{-}\sigma$  error bar is plotted in some panels. The dash-dot line at  $-3.0$  km/s corresponds to the radial velocity of the star.

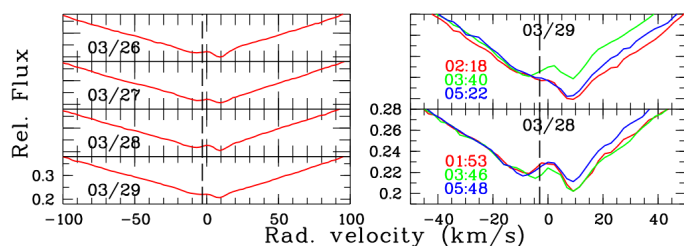


**Fig. 3.** Ca II K spectra obtained with the MPG/ESO 2.2 m telescope from March 26 to March 29. Right: average of the nightly spectra. Left: individual spectra taken during the nights March 28 and March 29. Colors correspond to the spectra obtained at different times (UT are shown).

night to night. Figure 2 shows the nightly residuals. The spectra of March 3 and 5 are close to the template one but there is a clear flux depression on March 4 and 6 at  $\sim 16$  km/s, the March 4, depth  $\sim 0.065$ , being deeper than the one on March 6, depth  $\sim 0.047$ . In both cases, a broad wing extending up to  $\sim 200$  km/s might be present. The corresponding Ca II H line depths are 0.052 and 0.047 for March 4 and 6, respectively.

*Mercator 2016 May.* Twenty spectra were taken consecutively along 4 hours on 2016 May 11. Figure 2 shows the Ca II K residuals with respect to the template spectrum grouped in four 1-hour periods. The residuals experience a smooth change in just 1-hour time and an event at  $\sim 9$  km/s develops achieving its deepest observed intensity of 0.068 depth during the last hour. A broad red wing seems to develop along the four observing hours.

*MPG/ESO 2016 March.* The Ca II K line exhibited a pronounced variation from night to night and within individual nights in timescales as short as less than 2 hours. No regular pattern can be inferred from the variations. Figure 3 shows the average of the spectra taken during each of the four nights. All nights show a distinct red-shifted event with respect to the template spectrum. Further, the strength of the events changes strikingly from one spectrum to another with time differences as short as 90 minutes. To exemplify this behaviour, Figure 3 shows the individual spectra from March 28 and March 29. Events at  $\sim 9$  km/s and depths as 0.118 (March 28) and 0.093 (March 29) are detected. There might exist some blue-shifted absorptions, at least in March 28, varying in velocity,  $-4$  to  $-9$  km/s, and tiny changes in the depth, 0.04–0.05.

## 5. Discussion

The variable absorptions at 10–20 km/s from the star, velocity dispersions  $\sim 10$ –20 km/s, depths  $\sim 0.05$ –0.1, and equivalent widths  $\sim 20$  mÅ, observed in  $\phi$  Leo behave similarly to the ones attributed to exocomets in  $\beta$  Pic. Nonetheless it is reasonable to consider other alternatives as a remarkable difference between both stars is that  $\phi$  Leo is not associated with a massive debris disk. This could be due to the age of  $\phi$  Leo as warm debris disks decline rapidly for stars older than a characteristic time of  $\sim 150$  Myr (Rieke et al. 2005). Also, as noticed before, it is unknown if the star is surrounded by a cold debris disk, which, in any case, declines rapidly for stars older than a characteristic time of  $\sim 400$  Myr (Su et al. 2006). Further, some relatively old stars with exocomets signatures do not possess a debris disks (Roberge & Weinberger 2008).

In the case of  $\beta$  Pic, phenomena involving the stellar atmosphere as the origin of the events were soon excluded (Lagrange–Henri et al. 1990). This seems also to be the case for  $\phi$  Leo since we would expect similar behaviour in other photospheric lines, which is not the case. Further, given the very short timescales of the variations, an origin in the interstellar medium is not plausible. Mass-loss rates resulting from weak radiatively driven winds in A stars are not expected to be significant around late-type A7IV stars, like  $\phi$  Leo. Such wind origin was excluded for  $\beta$  Pic (Lagrange–Henri et al. 1992) although it has not been for events in other stars (Redfield et al. 2007). Sporadic mass-loss events, i.e. clumps, generated in a hypothetical stellar wind and rotating with the star, or moving outwards with the wind, should produce emission lines moving from blue to red across the center of the line, or just be present in the blue and red wings of the wind lines. This is usually observed in relatively hot stars, like Be stars (Porter & Rivinius 2003). However, this behaviour is not observed in  $\phi$  Leo.

The ratio of the event depths observed in the Ca II K and H lines,  $\sim 1$ –1.5, differs from the oscillator strength ratio of these lines ( $=2$ ), suggesting that the variable absorptions arise from, at least partly, optically thick clumpy gas covering a small fraction of the stellar surface, again similar to  $\beta$  Pic or HD 172555 (Lecavelier des Etangs et al. 1997; Kiefer et al. 2014). These results, together with the high velocity broad line wings suggested in some spectra, makes it plausible that the  $\phi$  Leo events are traces of the evaporation of comet-like bodies in the CS en-

environment. In this scenario, the broad wings could be produced by a sort of comet-like coma or by several unresolved events.

Assuming a cometary origin, the similar dynamical properties of the events could point to a disruption of a larger primordial body by tidal forces in a near-star encounter, or to a family of comets (Beust et al. 1996) driven into the vicinity of the star by a planet. Several mechanisms not mutually exclusive from each other could deliver the bodies: Kozai-Lidov (Naoz 2016), secular resonances (Levison et al. 1994), mean motion resonances (Beust & Morbidelli 1996), or direct scattering by an eccentric planet (Beust et al. 1991). We note that only a future improvement of the event's statistics in  $\phi$  Leo will help to better constrain among the mentioned dynamical mechanisms. The orbit of the infalling bodies can only be roughly estimated since the radial velocity is degenerated between the pericenter distance and the angle formed between the axis of the orbit and the line of sight (true anomaly). Thus, the maximum pericenter distances where the bodies can originate (for a  $3.25 M_{\odot}$  star-estimated from the stellar parameters in section 2) is  $\sim 20$ -70 au. The observed infall velocities,  $\sim 0$ -20 km/s, maybe with some wings up to 200 km/s, are much lower than the free fall velocity at reasonable pericenter distances, 79 km/s and 177 km/s at 50 and  $10 R_{\star}$ , respectively. It seems that the most plausible option is that the presumable exocomets follow parabolic to hyperbolic orbits crossing the line of sight and in that case the main event absorption and the broad wings at larger velocities can be explained. The crossing distances must be close enough to the star to allow refractory material to sublimate. Following Beust et al. (1998), the minimum crossing distance would be  $\sim 0.21$  au using a FWHM of 20 km/s and assuming that the source of broadening the line is keplerian. Alternatively, if we assume thermal equilibrium (Beust et al. 1996) the distance at which dust sublimates, taking as a typical value  $T_{\text{sub}} = 1500$  K, would be  $\sim 0.46$  au or  $\sim 0.33$  au for albedos 0.0 and 0.5, respectively. Note that these values depend on the composition of the grains.

Concerning the Ca  $\pi$  “stable” component, we can exclude it arises in the local interstellar medium since interstellar lines are considerably narrower, the line of sight traverses the Leo cloud which has a centroid radial velocity of 1.75 km/s (Redfield & Linsky 2008), and its equivalent width gives a lower limit for the column density of  $N(H) \gtrsim 10^{20} \text{cm}^{-2}$ , much larger than the expected interstellar column densities in the Leo direction (Redfield & Linsky 2000). Thus, that component could arise in one of the scenarios suggested for the stable CS gas disk in  $\beta$  Pic - stellar winds, star-grazing comet evaporation, or grain evaporation near the star or in the disk (see Fernández et al. 2006) -, although we note that the  $\phi$  Leo “stable” component is broader and not as sharp as in  $\beta$  Pic (Lagrange-Henri et al. 1992). On the other hand, practically all stars showing the triangular shape rotate at very high velocities,  $v \sin i \gtrsim 200$  km/s. At these velocities the structure of the rotating stars and the inclination angle with respect to the line of sight affect their location on colour-magnitude diagrams (Bastian & de Mink 2009), and the induced oblateness of the star produces a gravity darkening resulting from the temperature gradient from the stellar equator to the poles. A preliminary test combining Kurucz models with a temperature gradient from the equator to the poles indicates that the strength of the triangular extra absorption decreases. A deeper analysis has been undertaken (Montesinos et al., in preparation).

## 6. Conclusions

Our intensive monitoring of  $\phi$  Leo that demonstrates its spectrum is very rich in red-shifted absorption events, which might be ac-

companied in some cases by broad wings and even blue-shifted absorptions. These sporadic events are similar to the ones in  $\beta$  Pic, and we find that the most plausible explanation is that they arise from exocomets grazing or falling onto the star. Assuming this scenario, it is intriguing how a relatively old, 500-900 Myr, star as  $\phi$  Leo without any known associated debris disk can possess such a rich environment hosting minor bodies. Another intriguing aspect refers to the origin of what it seems a triangular-shaped “stable” CS absorption component in the Ca  $\pi$  lines. Certainly, further monitoring is needed to better characterize the sporadic events as well as the stable component in comparison with similar stars.

*Acknowledgements.* Based on observations made with the Mercator Telescope, operated on the island of La Palma by the Flemish Community, at the Spanish Observatorio del Roque de los Muchachos of the Instituto de Astrofísica de Canarias. H.C., C.E., G. M., B. M., I. R., and E.V. are supported by Spanish grant AYA 2014-55840-P. J.O. acknowledges support from ALMA/Conicyt Project 31130027. O.A. is F.R.S.-FNRS Research Associate. We thank the referee H. Beust for his constructive comments.

## References

- Abt, H.A. 2008, ApJS 174, 499  
 Abt, H.A. 2015, PASP 127, 1218  
 Bastian, N., de Mink, S.E. 2009, MNRAS 398, L11  
 Beust, H., Lagrange-Henri, A.M., Vidal-Madjar, A., Ferlet, R. 1990, A&A 236, 202  
 Beust, H., Vidal-Madjar, A., Ferlet, R. 1991, A&A 247, 505  
 Beust, H., Lagrange, A.M., Plazy, F., Mouillet, D. 1996, A&A 310, 181  
 Beust, H., Lagrange, A.-M., Crawford, I. A., et al. 1998, A&A, 338, 1015  
 Beust, H., Morbidelli, A. 1996, Icarus 120, 358  
 David, T. J., Hillenbrand, L. A. 2015 ApJ 804, 146  
 de Bruijne, J.H.J., Eilers, A.-C 2012, A&A 546, A61  
 De Rosa, R. J.; Patience, J.; Wilson, P. A., et al. 2013, MNRAS 437, 1216  
 Ferlet, R., Hobbs, L.M., Vidal-Madjar, A. 1987, A&A 185, 267  
 Fernández, R., Brandeker, A., Wu, Y. 2006, ApJ 643, 509  
 Greaves, J. S., Holland, W. S., Matthews, B. C., et al. 2016, MNRAS, 461, 3910  
 Hobbs, L.M., Vidal-Madjar, A., Ferlet, R., Albert, C.E., Gry, C. 1985, ApJ 293, L29  
 Hughes, A., Wilner, D., Kamp, I., Hogerheude, M. 2008, ApJ, 681, 626  
 Jaschek, M., Jaschek, C., Andriolat, Y. 1988, A&A Suppl. 72, 505  
 Jaschek, Andriolat, Y., Jaschek 1988, A&A 250, 127  
 Kaufer, A., Stahl, O., Tubbesing, S., et al. 1999 The Messenger 95, 8  
 Kiefer, F., Lecavelier des Etangs, A., Augereau, J.-C. et al. 2014, A&A 561, L10  
 Kiefer, F., Lecavelier des Etangs, A., Boissier, J. 2015, Nature 514, 462  
 Lagrange-Henri, A.M., Ferlet, R., Vidal-Madjar, A. et al. 1990, A&A Suppl. 85, 1089  
 Lagrange-Henri, A.M., Gosset, E., Beust, H., Ferlet, R., Vidal-Madjar, A. et al. 1992, A&A 264, 637  
 Lecavelier des Etangs, A., Deleuil, M., Vidal-Madjar, A., et al. 1997, A&A 325, 228  
 Levison, H.F., Duncan, M.J., Wetherill, G.W. 1994, Nature 372, 441  
 Lieman-Sifry, J., Hughes, A. M., Carpenter, J. M., et al. 2016, ApJ, 828, 25  
 Marino, S., Matrà, L. Stark, C., et al. 2016, MNRAS, in press  
 Matthews, B.-C, Krivov, A.-V., Wyatt, M.-c., Bryden, G., Eiroa, C. 2014, Protostars and Planets, VI, 521.  
 Moór, A., Henning, T., Juhász, A., et al. 2015, ApJ, 814, 42  
 Naoz, S. 2016, arXiv 15601.07175  
 Olofsson, J., Juhász, A., Henning, T., Mutschke, H., Tamanai, A., Moór, A., Abrahám, P. 2012 A&A 542A, 900  
 Porter, J.M., Rivinius, T.H. 2003, PASP 115, 1153  
 Raskin, G., Van Winckel, H., Hensberge, H., et al. 2011, A&A, 526, A69  
 Redfield, S., & Linsky, J. L. 2000, ApJ, 534, 825  
 Redfield, S., Kessler-Silacci, J.E., Cieza, L.A. 2007, ApJ 661, 944  
 Redfield, S., & Linsky, J. L. 2008, ApJ, 673, 283-314  
 Rieke, G. H., Su, K. Y. L., Stansberry, J. A., et al. 2005, ApJ 620, 1010  
 Roberge, A. & Weinberger, A.J. 2008, ApJ 676, 509  
 Royer, F., Zorec, J., Gómez, A. E. 2007 A&A 463, 671  
 Su, K.Y.L., Rieke, G.H., Stansberry, J.A., et al. 2006, ApJ 653, 675  
 Welsh, B.Y., & Montgomery, S.L., Advances in Astronomy, Vol. 2015  
 Zorec, J., Royer, F. 2012, A&A 537, A120  
 Zuckerman, B., Song, I. 2012, ApJ 758, 77

- 
- <sup>1</sup> Dpto. Física Teórica, Universidad Autónoma de Madrid, Cantoblanco, 28049 Madrid, Spain, e-mail: [carlos.eiroa@uam.es](mailto:carlos.eiroa@uam.es)
  - <sup>2</sup> CAB (CSIC-INTA), Camino Bajo del Castillo, s/n, 28692 Villanueva de la Cañada, Madrid, Spain
  - <sup>3</sup> STAR Institute, Université de Liège, F.R.S.-FNRS, 19c Allée du Six Août, B-4000 Liège, Belgium
  - <sup>4</sup> Max-Planck-Institut für Astronomie (MPIA), Königstuhl 17, D-69117 Heidelberg, Germany
  - <sup>5</sup> Instituto de Física y Astronomía, Facultad de Ciencias, Universidad de Valparaíso, 5030 Casilla, Valparaíso, Chile
  - <sup>6</sup> Université de Toulouse, UPS-OMP, IRAP, Toulouse F-31400, France
  - <sup>7</sup> Space Telescope Science Institute, 3700 San Martin Drive, Baltimore, MD 21212, USA
  - <sup>8</sup> Steward Observatory, Department of Astronomy, University of Arizona, Tucson, AZ 85721, USA
  - <sup>9</sup> INAF, Osservatorio Astronomico di Palermo, 90134 Palermo, Italy
  - <sup>10</sup> Konkoly Observatory, Research Centre for Astronomy and Earth Sciences, PO Box 67, 1525 Budapest, Hungary
  - <sup>11</sup> Aurora Technology B.V. for ESA, ESA-ESAC, Camino Bajo del Castillo, s/n, 28692 Villanueva de la Cañada, Madrid, Spain
  - <sup>12</sup> Lund Observatory, Department of Astronomy and Theoretical Physics, Lund University, Box 43, SE-221 00 Lund, Sweden
  - <sup>13</sup> ESA-ESAC, Camino Bajo del Castillo, s/n, 28692 Villanueva de la Cañada, Madrid, Spain
  - <sup>14</sup> Exoplanets & Stellar Astrophysics Lab, NASA Goddard Space Flight Center, Code 667, Greenbelt, MD 20771, USA